KFUPM
Journal of Undergraduate Research International

Diamond Open Access 15

Article Chemical Engineering

# Thermochemical Conversion of $H_2S$ to Hydrogen: A Techno-Economic Assessment

Zainab Al Abdrabalnabi and Umer Zahid*

Cite https://doi.org/10.64589/juri/231611

**Submitted:** April 25, 2026 **Revised:** May 27, 2026 **Accepted:** June 07, 2026

**ABSTRACT**

The increasing demand for clean hydrogen production and sustainable utilization of sour gas resources has motivated the development of alternative processes beyond conventional technologies. In this study, two hydrogen production pathways, hydrogen sulfide ($H_2S$) thermal splitting and hydrogen sulfide methane reforming ($H_2SMR$), were modeled and compared using Aspen Plus under realistic operating conditions. Rigorous simulations incorporating both thermodynamic and kinetic approaches were developed to evaluate process performance in terms of energy efficiency and economic feasibility. The results indicate that $H_2SMR$ exhibits superior energy performance, with a specific energy consumption of approximately 51 kWh/kg, compared with 98 kWh/kg for $H_2S$ thermal splitting, corresponding to an improvement of nearly 50%. This enhancement was attributed to the synergistic effect of methane in promoting hydrogen production and improving energy utilization. However, $H_2SMR$ requires a considerably higher capital investment ($88.5 million) compared with $H_2S$ splitting ($42.7 million), primarily because of increased equipment costs, particularly of compressors and reactors. In addition, $H_2SMR$ exhibits higher operating costs, driven by elevated utility consumption resulting from the large recycling stream caused by low reactor conversion. The hydrogen production costs were estimated to be $2.25/kg for $H_2SMR$ and $2.78/kg for $H_2S$ thermal splitting. Although the $H_2S$ thermal splitting process offers improved energy efficiency, the $H_2SMR$ design presents an economically favorable option under the studied conditions. These findings highlight the tradeoff between the energy performance and economic viability of hydrogen production from sour gas streams.

**Keywords:** hydrogen, techno-economics, H2S, process simulation, resource utilization

## 1. INTRODUCTION

Natural gas is a hydrocarbon resource that is used worldwide for various purposes, such as mobility, manufacturing, and energy generation. Global natural gas production reached 4.19 trillion cubic meters and consumption increased by approximately 2.8% in 2024 compared with the previous year, largely supported by industry and electricity generation [1]. Before being utilized in power generation, industrial processes, or domestic uses, natural gas must undergo a series of processing steps to meet certain product specifications. These processes include separation to remove unwanted liquids, such as produced water, and hydrocarbon condensates (e.g., propane, butane, and heavier components that condense under surface conditions). They also remove solid particles such as sand, clay, scale, corrosion products, and other formation debris carried from the reservoir. Subsequently, sweetening eliminates acidic gases such as hydrogen sulfide ($H_2S$) and carbon dioxide ($CO_2$), and dehydration removes water vapor to prevent corrosion and hydrate formation, ensuring that the gas meets the pipeline specifications. Natural gas processing also requires energy input across various processes and can produce toxic byproducts. With increasing global reliance on natural gas, exploring optimal and sustainable approaches for its processing and utilization has become a necessity. Natural gas extracted from reservoirs typically contains impurities, such as $CO_2$, $H_2S$, and water, which must be treated prior to use. Hydrogen ($H_2$), derived from natural gas, plays a critical role in several sectors, including transportation, manufacturing, and energy systems. Currently, steam methane reforming is the most widely used hydrogen production technology. However, it leads to considerable $CO_2$ emissions, raising environmental concerns and motivating the investigation of alternative hydrogen production pathways.

In refineries and gas processing plants, the $H_2S$ present in natural gas is treated as an undesirable impurity and is removed through conventional processing methods. A widely used approach is the Claus process, in which $H_2S$ is converted into elemental sulfur. During this process, the $H_2$ content of $H_2S$ is ultimately lost in the form of water, indicating that current industrial techniques primarily focus on $H_2S$ removal and disposal rather than its utilization. These approaches are primarily designed to address environmental and safety concerns, while overlooking the potential of $H_2S$ as a valuable resource. This highlights the need to explore alternative processes that consider broader objectives beyond environmental compliance, such as utilizing this toxic gas for hydrogen


Published under an exclusive license by KFUPM

production through processes such as $H_2S$ thermal splitting and reforming.

Alternative hydrogen production methods that treat $H_2S$ and natural gas components as resources rather than as waste streams have been explored, including high-temperature thermochemical catalytic decomposition, plasma-assisted cracking, electrochemical oxidation in specialized cells, and photocatalytic splitting under light irradiation. In addition, integrated reforming routes combine $H_2S$ with methane to enhance hydrogen yield. Despite differences in energy input and operating conditions, these approaches convert sour gas components into $H_2$ and elemental sulfur without the direct $CO_2$ emissions associated with conventional reforming processes. For $H_2S$ splitting, thermochemical decomposition over nickel sulfide catalysts showed that surface reactions dominate $H_2$ formation at moderate temperatures, confirming the feasibility of $H_2$ recovery from $H_2S$ through cyclic sulfurization–regeneration processes[2]. To overcome these equilibrium limitations, membrane-assisted packed-bed reactors have been developed to selectively remove $H_2$, considerably enhancing $H_2S$ conversion compared with conventional reactor configurations[3]. Biomass-derived sulfur compounds generate substantial amounts of $H_2S$ under steam-assisted conditions, indicating that $H_2S$ formation is more widespread than previously assumed, reinforcing the need for utilization-based strategies rather than disposal[4]. Plasmonic photocatalysis has recently emerged as a low-temperature, $CO_2$-free route for direct $H_2S$ decomposition, achieving enhanced hydrogen production under visible-light irradiation[5]. Building on these approaches, Dogan et al.[6] demonstrated that sawdust-based activated carbon, which is a catalyst and support for iron (Fe) and tungsten (W) catalysts, enabled $H_2S$ conversion close to thermodynamic equilibrium, with $CS_2$, CO, and $CO_2$ formed as minor byproducts. It highlighted the potential of biomass-derived materials for efficient hydrogen production and waste valorization.

Beyond direct $H_2S$ splitting, hydrogen sulfide methane reforming ($H_2SMR$) has been investigated as a pathway for simultaneous hydrogen production and sulfur valorization. Thermodynamic analyses revealed that $H_2S$ considerably influenced the reaction equilibrium, hydrogen yield, and carbon suppression[7]. Process simulation studies have emphasized that the $CH_4/H_2S$ feed ratio and operating temperature are critical for hydrogen yield, carbon deposition, and separation energy requirements, demonstrating competitive economics when sulfur-containing byproducts, such as elemental sulfur and carbon disulfide, are recovered[8]. Kinetic and techno-economic analyses further indicated that the radicals generated from $H_2S$ decomposition enhanced methane conversion, with moderate feed ratios optimizing $H_2$ and carbon disulfide production[9]. Additional thermodynamic studies have proposed integrated process schemes combining reactions, byproduct recovery, and $H_2$ compression to improve overall efficiency[10]. Life cycle assessments confirmed that $H_2SMR$ reduces global warming impacts compared with conventional steam methane reforming, although energy-intensive separation steps and material use remain key challenges that require mitigation[8].

Despite extensive thermodynamic and catalytic studies on $H_2S$ splitting and $H_2SMR$, existing literature largely focuses on equilibrium-based analyses and laboratory-scale observations. However, limited attention has been paid to realistic process conditions, full-process integration, and downstream separation requirements. Sulfur-containing byproducts are commonly treated as secondary streams without rigorous evaluation of their recovery, purity, or economic value. $H_2S$ thermal pyrolysis, despite its potential for direct hydrogen production, remains underexplored at the process level owing to unquantified perceived energy penalties. Consequently, comprehensive process simulations and comparative assessments of $H_2S$ splitting and $H_2SMR$ under realistic operating conditions are still lacking. In this study, two hydrogen production routes, $H_2S$ thermal splitting and $H_2SMR$, were modeled in Aspen Plus using both kinetic and thermodynamic approaches. Rigorous process simulations were developed to consistently compare the two processes in terms of safety, environmental impact, and economic performance under realistic operating conditions.

## 2. PROCESS DESCRIPTION

**2.1. Case 1: $H_2S$ Thermal Splitting.** Hydrogen sulfide thermal splitting was employed as the primary reaction pathway for hydrogen production. In this process, $H_2S$ undergoes high-temperature thermal decomposition, as shown in Eq. 1.

$$H_2S \rightarrow H_2 + \frac{1}{2}S_2 \quad \Delta H^\circ = +90\,\mathrm{kJ \cdot mol^{-1}} \tag{1}$$

The process flow diagram (PFD) for the $H_2S$ thermal splitting process is shown in Figure 1, illustrating the main equipment and process streams. The $H_2S$ splitting reaction is strongly endothermic; therefore, it typically occurs at elevated temperatures in the range of 800–1500 °C[11]. To achieve the required reaction temperature while improving energy efficiency, the $H_2S$ feed stream was preheated using a heat exchanger, where thermal energy from the hot reactor effluent was recovered and transferred to the incoming feed. The preheated stream was then introduced into a high-temperature reactor (R-101) where thermal decomposition occurred. The reactor effluent consisted primarily of $H_2$, sulfur vapor ($S_2$), and unreacted $H_2S$. This stream was subsequently directed to a separation unit (SPL-101), where sulfur was recovered by cooling the stream to condense the sulfur vapor, enabling its recovery in a solid form, which is preferred for industrial handling and storage. The remaining gas stream, primarily composed of $H_2$ and residual $H_2S$, was then cooled and compressed prior to entering an absorption column (ABS-101). In the absorber, an aqueous methyldiethanolamine (MDEA) solution was used as the solvent to selectively absorb $H_2S$ from the gas mixture, allowing $H_2$ to exit from the top of the column, where the overhead stream primarily contained $H_2$ with a small amount of water, which is typically removed using dehydration methods such as molecular sieves. The rich solvent stream containing the absorbed $H_2S$ was withdrawn from the bottom of the absorber and sent to a regeneration column (STR-101), where thermal regeneration was applied to release the absorbed $H_2S$. The regenerated $H_2S$ stream was recycled to the process feed, whereas the lean MDEA solution was recycled to the absorber after appropriate cooling to maintain suitable absorption conditions. To enhance the overall energy efficiency of the process, heat integration was implemented in the regeneration section, in which the hot stream leaving the bottom of the regeneration

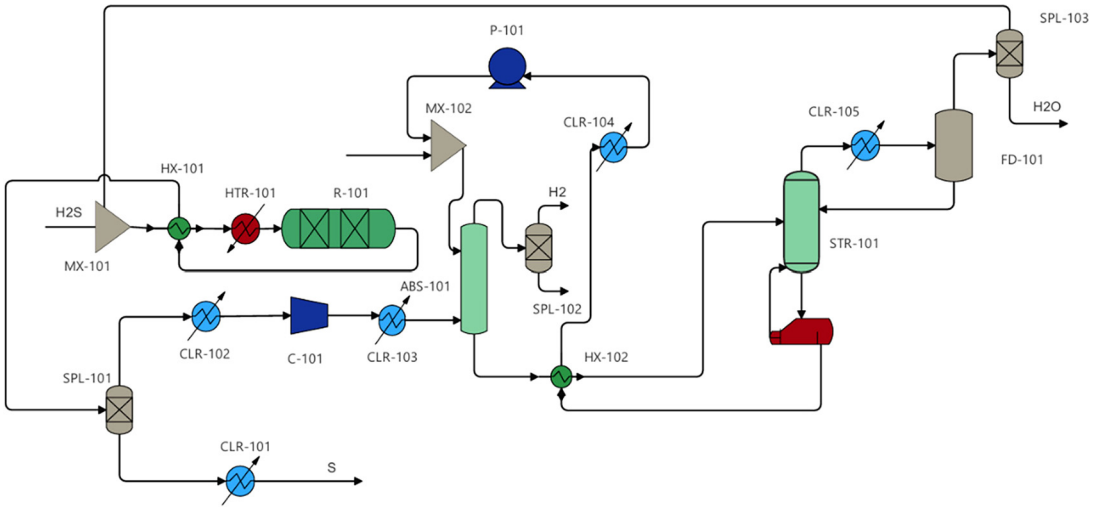



**Figure 1.** Process flow diagram for $H_2S$ splitting to $H_2$

column was used to preheat the incoming rich solvent stream, thereby reducing the external heating and cooling requirements of the system.

**2.2. Case 2: $H_2S$ Methane Reforming ($H_2SMR$).** In this process, $H_2SMR$ was used to produce $H_2$, in which methane and $H_2S$ reacted at high temperatures, as shown in Eq. 2.

$$2H_2S + CH_4 \rightarrow CS_2 + 4H_2 \quad \Delta H^\circ = +232.4\,\text{kJ} \cdot \text{mol}^{-1} \tag{2}$$

The reaction is highly endothermic, and based on the kinetic study, a $CH_4$:$H_2S$ molar ratio of 1:12 and a temperature range of 749.85–1049.85 °C were used, with the reaction occurring over a zirconia catalyst modified with lanthanum oxide and impregnated with molybdenum [12]. Methane and $H_2S$ were first mixed and preheated using a heat exchanger (HX-101) and then introduced into a high-temperature reactor (R-101) where the reaction occurred. The reactor effluent was subsequently used to preheat the incoming feed before being sent to a separation unit (SPL-101) to remove sulfur, following which the stream was directed to a distillation column (DC-101) to separate the liquid $CS_2$. The remaining stream was compressed and cooled to enhance the absorption efficiency before entering the absorption column (ABS-101), where a solvent stream containing water and MDEA was introduced. The overhead stream primarily contained $H_2$ with a small amount of water, which is typically removed using dehydration methods, such as molecular sieves. The bottom stream from the absorber was sent to a regeneration column (STR-101) to remove the remaining $H_2S$, which was recycled to the feed, whereas the regenerated solvent was recycled to the absorber. Before entering the regeneration column, the rich stream was heated using a heat exchanger (HX-102) by exchanging heat with the hot bottom stream of the column, which reduced the cooling duty required for the solvent recycling stream. The PFD for the $H_2SMR$ process is shown in Figure 2, which illustrates the main equipment and process streams.

## 3. SIMULATION METHODOLOGY

The $H_2S$ thermal splitting process and the $H_2SMR$ process were simulated using Aspen Plus V14 under steady-state conditions while assuming a zero pressure drop throughout the system. The IDEAL property method was used for most of the process units, whereas the ELECNRTL property method was selected for the absorption sections owing to the presence of the aqueous MDEA system. For the $H_2S$ thermal splitting process, the feed consisted of pure $H_2S$ at 50 °C and 101.3 kPa. The feed was first preheated using a heat exchanger by recovering heat from the reactor effluent before entering a plug-flow reactor (PFR, R-101), where a power-law kinetic model based on literature data was applied, as shown in Eq. 3. To validate the reactor performance, an RGIBBS reactor was initially used to estimate the maximum equilibrium conversion, which was approximately 82% [11], and the PFR dimensions were then adjusted to approach this value. The reactor effluent primarily contained $H_2$, sulfur vapor and unreacted $H_2S$. Elemental sulfur was used in Aspen instead of $S_2$ because of property limitations. It was separated using an SEP block (SPL-101), then cooled to 110 °C to obtain solid sulfur. The remaining stream containing $H_2$ and $H_2S$ was

**Table 1.** *Mass balance of the major process streams for the $H_2S$ splitting process*

| Stream | Temperature (°C) | Pressure (bar) | Mole Flow (kmol/h) | Mass Flow (kg/h) | $H_2$ | $H_2S$ | S |
|---|---|---|---|---|---|---|---|
| Feed ($H_2S$) | 50 | 1 | 700 | 23857.3 | 0 | 1 | 0 |
| Reactor Outlet | 1250 | 1 | 1525.5 | 28142.4 | 0.5 | 0.1 | 0.5 |
| $H_2$ Product | 40.3 | 5 | 699.7 | 1410.6 | 1 | 0 | 0 |
| Recycle | 30 | 1 | 125.7 | 4285.2 | 0 | 1 | 0 |

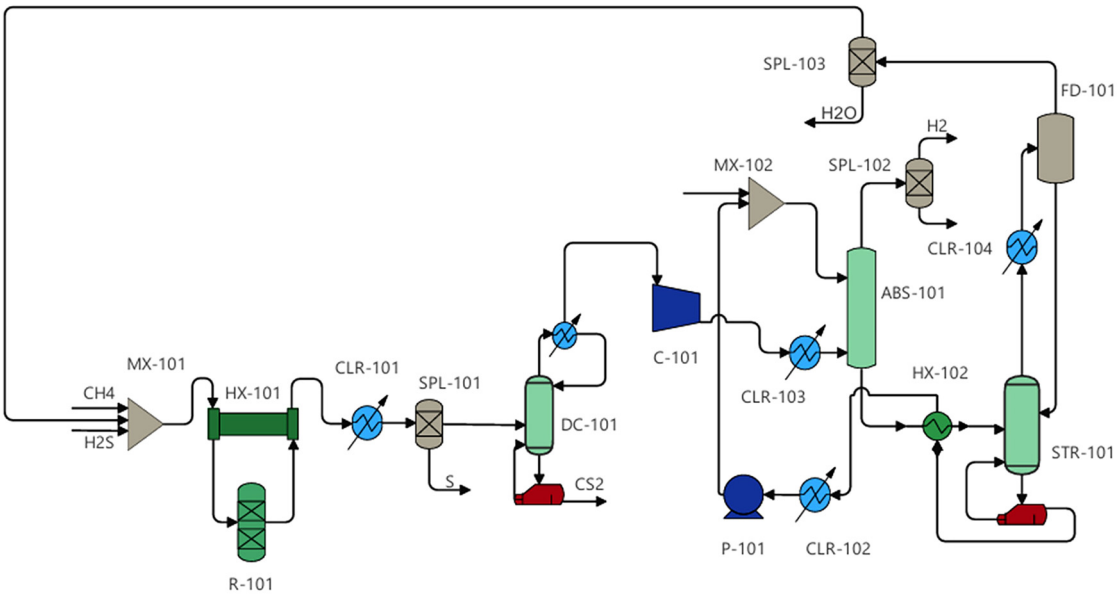



**Figure 2.** Process flow diagram for $H_2S$ reforming ($H_2SMR$) to $H_2$

cooled, compressed to 5 bar, and further cooled to 40 °C before entering an absorber (ABS-101) with 25 stages. A second stream containing water and MDEA was introduced, where $H_2S$ was absorbed and $H_2$ was recovered as the overhead product with approximately 100% purity; water was removed in the simulation using a separator (SPL-102), while in practice, a molecular sieve was used. The bottom stream of the absorber was sent to a regeneration column (STR-101), where $H_2S$ was removed from the top and recycled back to the feed, while the regenerated solvent was recycled after cooling. A heat exchanger (HX-102) was used before the regeneration column to preheat the feed using hot regeneration column bottoms, thereby reducing the cooling duty of the solvent recycling stream.

$$-r = 2 \times 10^{11} \exp\left(\frac{-274.4}{RT}\right) \quad (3)$$

For the $H_2SMR$ process, the feed consisted of $CH_4$ and $H_2S$ in a molar ratio of 1:12 at 50 °C and 101.3 kPa. The streams were mixed (MX-101), preheated (HX-101), and sent to an RGIBBS equilibrium reactor (R-101), where the methane conversion reached approximately 99% and the $H_2S$ conversion was approximately 25%. The reactor effluent was used to preheat the feed before it was sent to a separator (SPL-101) to remove sulfur, followed by a distillation column (DC-101) to separate the liquid $CS_2$. The column bottom contained pure $CS_2$, while the overhead stream, consisting of $H_2$ and $H_2S$, was compressed to 5 bar and cooled to 40 °C before entering an absorber (ABS-101) with 25 stages. A solvent stream containing MDEA and water was introduced, producing $H_2$ as the overhead stream with a small amount of water, which was removed in Aspen using a separator (SPL-102), but would typically be removed using a molecular sieve in the industry. The bottom stream of the absorber, containing $H_2S$ and solvent, was sent to a regeneration column (STR-101), where $H_2S$ was removed from the top and recycled back to the feed. The regenerated solvent from the regeneration column bottom was cooled to 40 °C and recycled into the absorber. Additionally, a heat exchanger (HX-102) was placed before the regeneration column, and the hot regeneration column bottom stream was used to heat the incoming feed, reducing the cooling duty required for the solvent recycling stream.

## 4. MODEL VALIDATION

The simulation results were first validated for the $H_2S$ thermal decomposition process by comparing the predicted $H_2S$ conversion with values reported in the literature[13]. The model was based on thermodynamic equilibrium using Gibbs free energy minimization for the H–S–N system. According to the literature, limited $H_2S$ decomposition occurs at low temperatures owing to equilibrium constraints, with conversions remaining below 5% even up to approximately 850 °C. However, at higher temperatures above 1200 °C, the reaction becomes rapid and approaches equilibrium, with reported conversions in the range of 79–82%[11].

**Table 2.** *Mass balance of the major process streams for the $H_2SMR$ process*

| Stream | Temperature (°C) | Pressure (bar) | Mole Flow (kmol/h) | Mass Flow (kg/h) | $H_2$ | $H_2S$ | S | $CS_2$ | $CH_4$ |
|---|---|---|---|---|---|---|---|---|---|
| Feed ($CH_4$) | 50 | 1 | 347.1 | 5568.1 | 0 | 0 | 0 | 0 | 1 |
| Feed ($H_2S$) | 50 | 1 | 700 | 23857.3 | 0 | 1 | 0 | 0 | 0 |
| Reactor Outlet | 1049.9 | 1 | 5205.3 | 147517.8 | 0.3 | 0.7 | Trace | 0.1 | Trace |
| $H_2$ Product | 40.4 | 5 | 1386.5 | 2795 | 1 | 0 | 0 | 0 | 0 |
| Recycle | 22.8 | 1 | 3465 | 118092.2 | 0 | 1 | 0 | 0 | 0 |

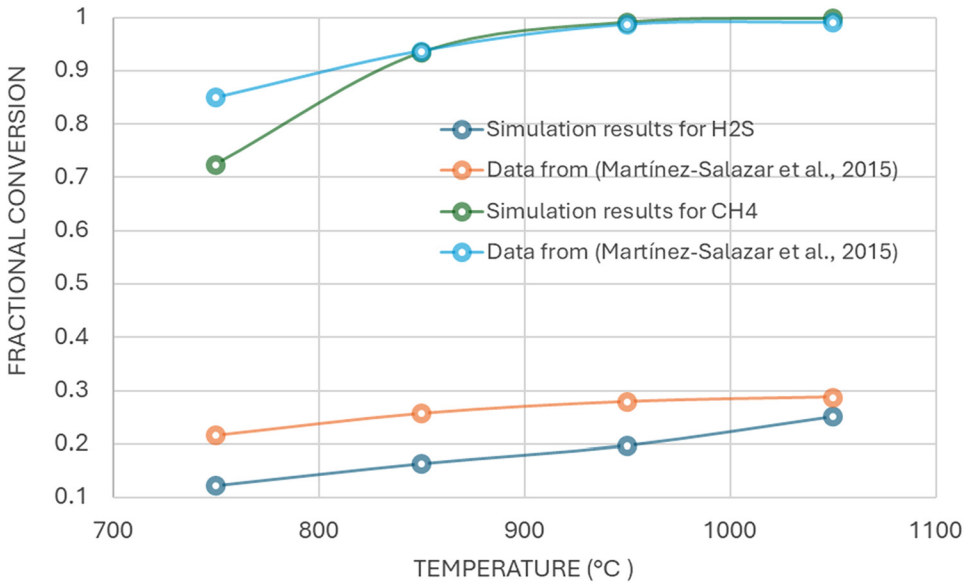



**Figure 3.** Validation of $CH_4$ and $H_2S$ conversion as a function of temperature

In this study, the simulation achieved an $H_2S$ conversion of 82%, which falls within the reported equilibrium range of 79–82%. Therefore, the model is reliable and accurately represents the high-temperature decomposition behavior of $H_2S$.

After validating the decomposition, the model was further validated for the $H_2S$ reforming process.

The developed model was validated against the literature data for both $CH_4$ and $H_2S$ conversion at different temperatures under consistent operating conditions. As shown in Figure 3, the model predictions closely follow the literature trend for $CH_4$ conversion, which increases considerably with temperature, rising from approximately 0.93 at 750 °C to nearly 0.99 at 1050 °C. This behavior was expected owing to the endothermic nature of the reforming reaction, in which higher temperatures enhance the reaction rate and improve the conversion. The agreement between the model and literature values for methane is reasonable, with minor deviations that may be attributed to ideal reactor behavior and neglecting transport limitations. For $H_2S$ conversion, the model also captures an increasing trend with temperature, with conversion rising from approximately 0.12 at 750 °C to approximately 0.25 at 1050 °C. However, compared with methane, the agreement with literature data is less precise, with noticeable deviations across the temperature range. This is attributable to the more complex reaction behavior

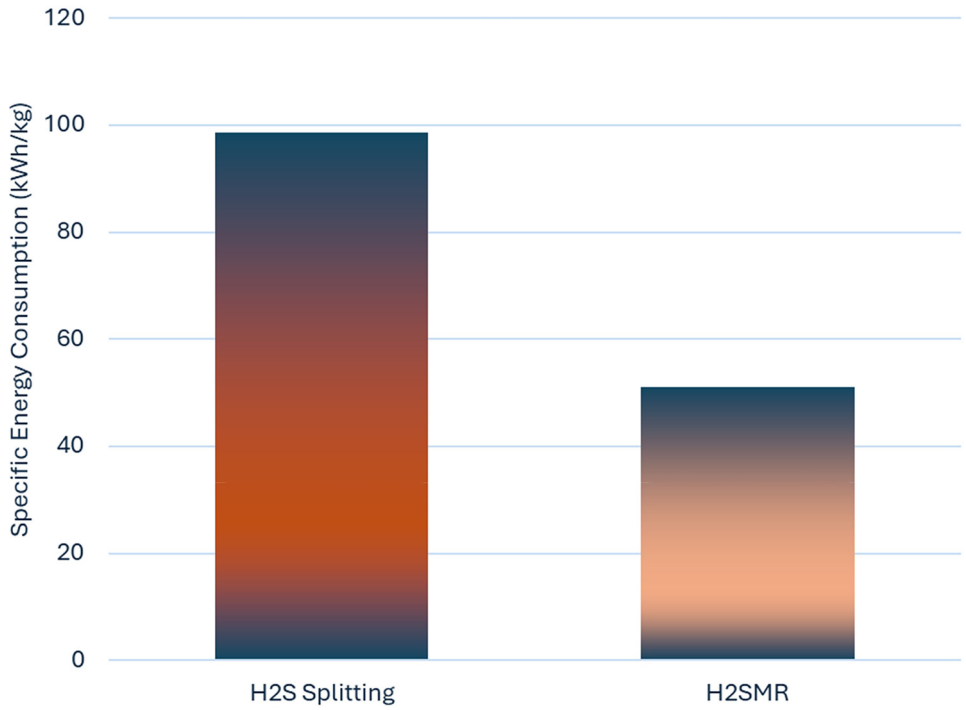



**Figure 4.** Specific energy consumption (SEC) for $H_2S$ splitting and $H_2S$MR processes

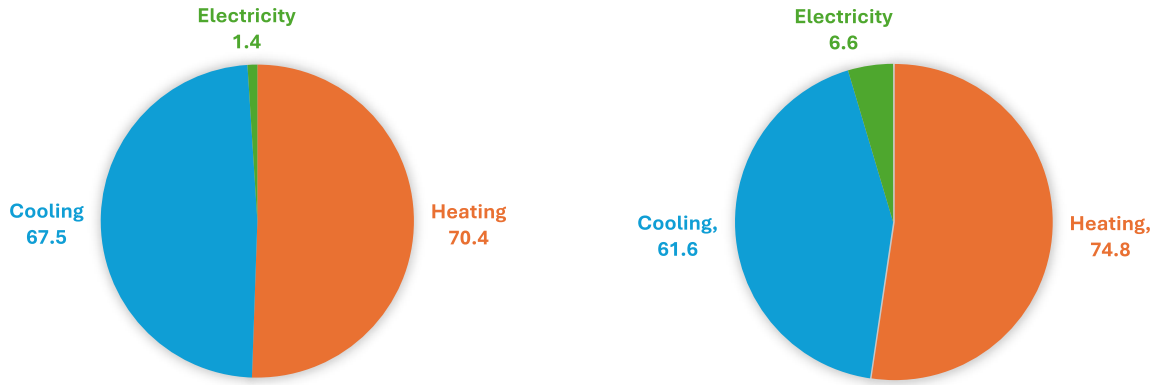



**Figure 5.** a. Utility distribution for the $H_2S$ decomposition process in MW b. Utility distribution for the $H_2S$MR process in MW

of $H_2S$, possible side reactions, and limitations in the kinetic representation. Additionally, assumptions such as ideal reactor behavior and neglecting the mass and heat transfer effects may contribute to these differences. Overall, the model demonstrated high accuracy in predicting methane conversion and acceptable performance for $H_2S$ conversion, thereby capturing the general temperature-dependent behavior of the system.

## 5. RESULTS AND DISCUSSION

**5.1. Energy Analysis.** The energy performance of the process was evaluated using specific energy consumption (SEC), defined as the energy required per unit of $H_2$ produced. SEC is a key indicator of process efficiency, with lower values corresponding to more energy-efficient systems. As shown in Figure 4, the SEC of the $H_2S$ splitting process was approximately 98 kWh/kg, whereas the $H_2S$MR process required considerably lower energy, with an SEC of approximately 51 kWh/kg. This indicates that the $H_2S$MR process is nearly 50% more energy-efficient than direct $H_2S$ decomposition. The higher energy demand in the splitting process is primarily because of the extreme temperatures required for the endothermic decomposition reaction and overcoming the equilibrium limitations. By contrast, methane enhances hydrogen production through reforming reactions and improves overall energy utilization in the $H_2S$MR process. Consequently, lower external energy is required per unit of $H_2$ produced.

To further understand the energy distribution, utility consumption was analyzed for both processes. For the $H_2S$ splitting process, heating accounted for approximately 51% of the total utility demand, followed by cooling at 48%, whereas electricity contributed only approximately 1%. This reflects the high thermal requirements of the process, in which considerable heat input is required to maintain high reaction temperatures, along with substantial cooling for downstream processing. Similarly, in the $H_2S$MR process, heating remained the dominant utility at approximately 52%, with cooling contributing 43%, and electricity contributing approximately 5%. Compared with $H_2S$ splitting, the slightly higher electricity usage may be associated with additional unit operations, such as compression. However, the overall energy demand remains low owing to the improved reaction efficiency. Overall, the results indicate that although both processes are thermally intensive, $H_2S$MR exhibits a higher energy efficiency (32%) than $H_2S$ splitting (22%), as reflected

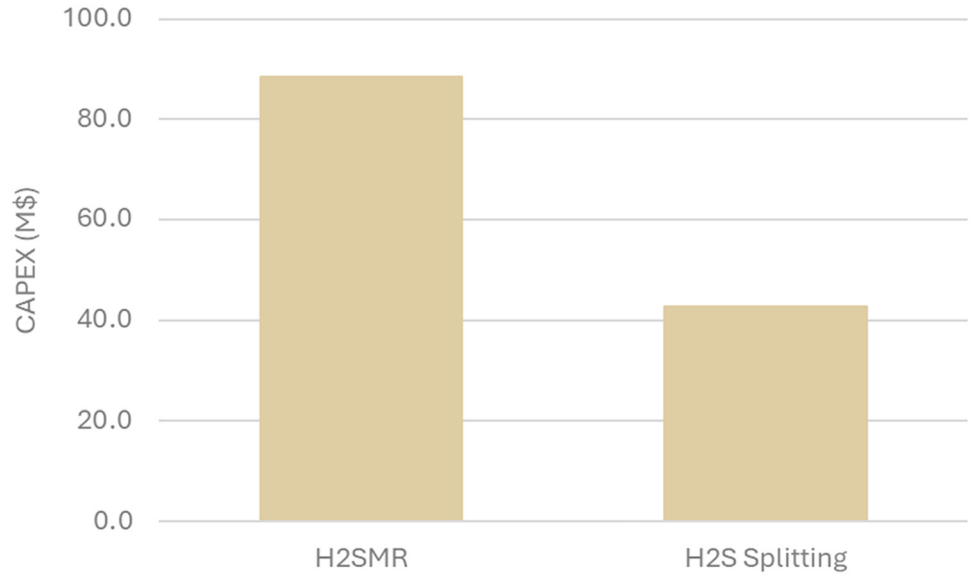



**Figure 6.** Comparison of total capital cost (CAPEX) for $H_2S$MR and $H_2S$ splitting processes

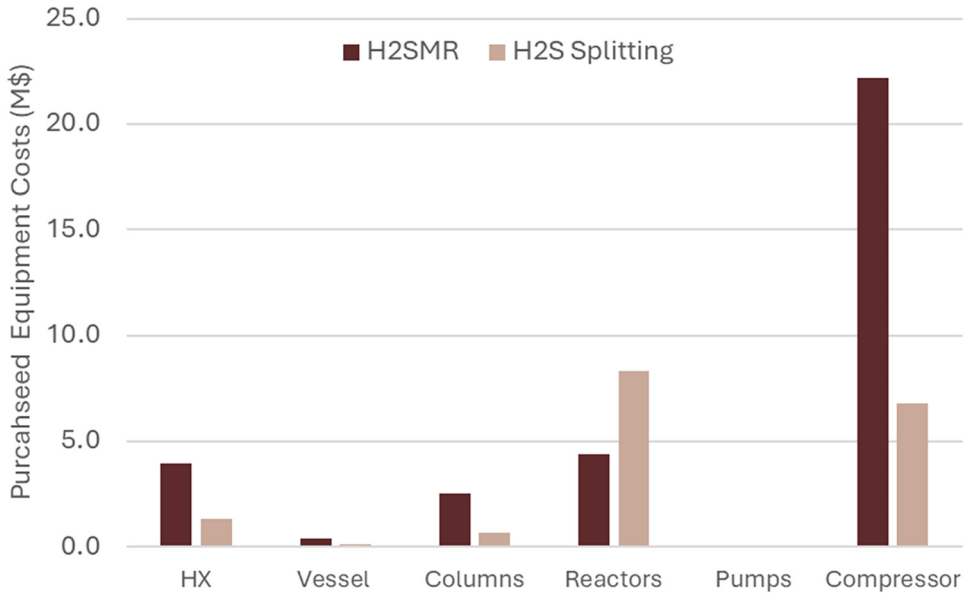



**Figure 7.** Purchased equipment cost distribution for $H_2$SMR and $H_2$S splitting processes

by its lower SEC. This makes it more favorable from an energy perspective under the studied conditions.

**5.2. Cost Analysis.** The economic performance of the $H_2$SMR and $H_2$S splitting processes was evaluated based on capital investment and operating cost distribution. A detailed breakdown of the equipment costs and operating cost components was performed to identify the key contributors affecting the overall process economics. As shown in Figure 6, the $H_2$SMR process requires a substantially higher capital investment ($88.5 million) compared with $H_2$S splitting ($42.7 million). The $H_2$SMR-based configuration is more equipment-intensive, reflecting its higher design complexity and infrastructure requirements. By contrast, the $H_2$S splitting process is a more economically attractive option from an initial investment perspective.

The distribution of purchased equipment costs is shown in Figure 7. Compressors contribute the largest share of capital costs to the $H_2$SMR process, followed by reactors and heat exchangers. The high compressor cost is a key factor driving the overall CAPEX of $H_2$SMR. For $H_2$S splitting, the cost distribution is more balanced, with reactors representing a relatively higher contribution than other equipment. Overall, the reduced cost intensity across major equipment explains the lower total CAPEX for the $H_2$S splitting process.

Figure 8 illustrates the contributions of the different components to the total operating cost. Utilities represent the dominant cost in both processes, followed by raw material expenses, whereas labor and maintenance make relatively minor contributions. The $H_2$SMR process has higher utility and raw material costs than $H_2$S splitting, indicating a more energy and resource-intensive operation owing to larger recycle streams.

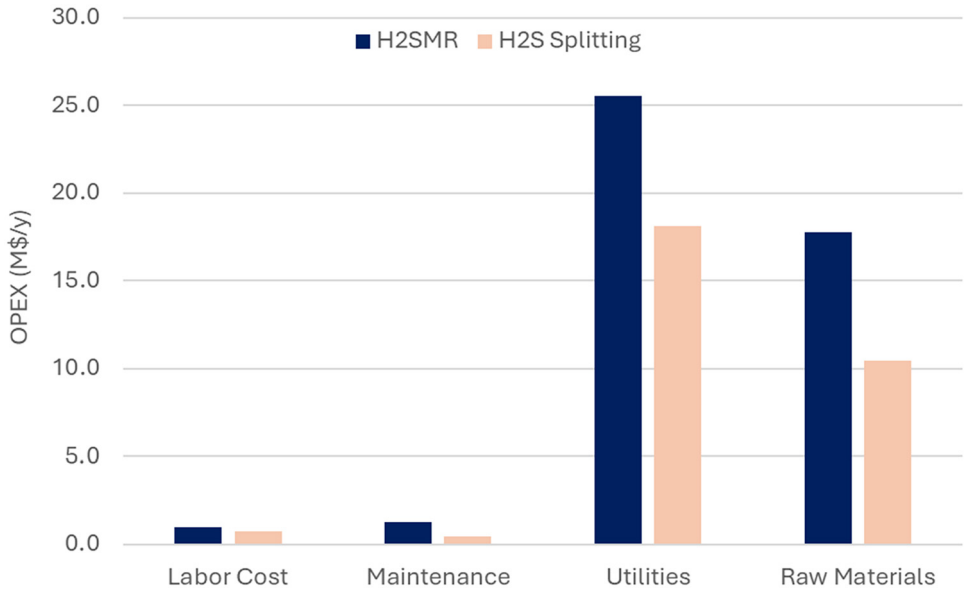



**Figure 8.** Operating cost breakdown for $H_2$SMR and $H_2$S splitting processes

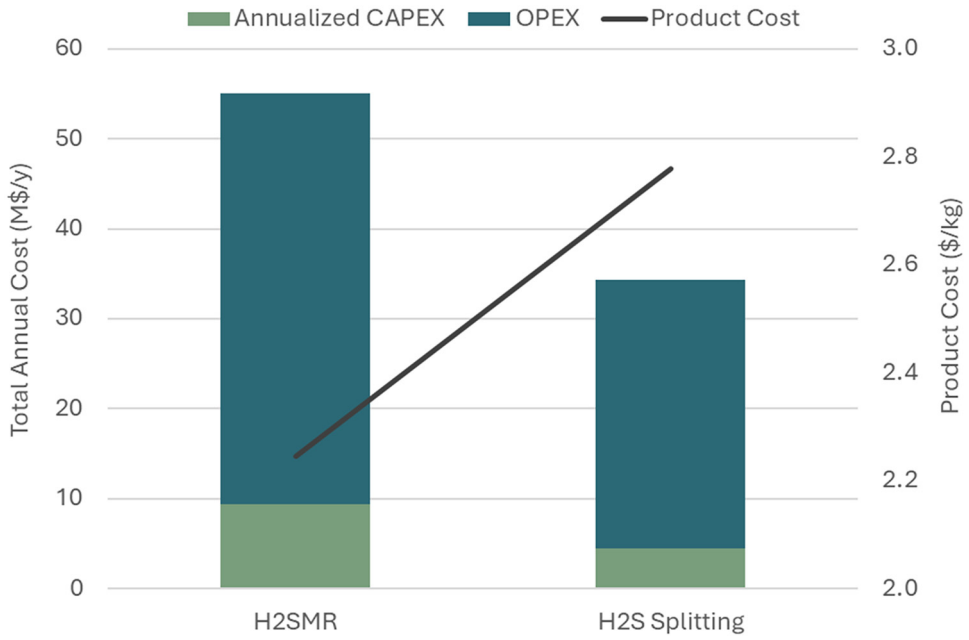



**Figure 9.** Total annual cost (TAC), annualized CAPEX, OPEX, and product cost comparison

This trend highlights the impact of process conditions and energy demand on operating expenditures.

The overall economic performance is summarized in Figure 9 by comparing the annualized CAPEX, OPEX, and product costs. The $H_2S$MR process has higher operating costs, which dominate the total annual cost (TAC), despite its moderate annualized capital contribution. By contrast, $H_2S$ splitting achieves a lower TAC owing to lower capital and operating expenses. Although $H_2S$MR has higher CAPEX and OPEX than the $H_2S$ splitting process, its higher process efficiency and better productivity result in a lower per-unit cost of $H_2$. These results indicate that the product cost of $H_2$ is lower in the $H_2S$MR process, confirming its economic advantage, and the operating cost, particularly utilities, is the primary driver of total cost in both cases.

## 6. CONCLUSIONS

This paper presents a comparative assessment of hydrogen production from $H_2S$ through thermal splitting and $H_2S$MR using a rigorous process simulation. The analysis incorporated model validation, energy evaluation, and a detailed economic assessment to provide a comprehensive understanding of both processes under realistic operating conditions. The simulation results confirmed that $H_2S$MR offered superior energy performance with considerably lower specific energy consumption than $H_2S$ thermal splitting, reaching approximately 51 kWh/kg for $H_2S$MR and 98 kWh/kg for $H_2S$ thermal splitting. This improvement was primarily owing to the contribution of methane in enhancing hydrogen yield and reducing the external energy requirement. The utility analysis further indicated that both processes were energy-intensive, with heating and cooling representing the dominant energy demands. From an economic standpoint, the results showed that $H_2S$MR required a substantially higher capital investment owing to the cost of major equipment, particularly compressors and reactors, with a total capital investment of $88.5 million compared with $42.7 million for $H_2S$ thermal splitting. The operating costs of $H_2S$MR were higher, driven primarily by the increased utility consumption and raw material usage. Consequently, the TAC of $H_2S$MR exceeded that of $H_2S$ thermal splitting. By contrast, $H_2S$ thermal splitting demonstrated a lower capital investment and reduced operating costs, but with a lower hydrogen production rate. Overall, the findings indicate that $H_2S$MR is more favorable from an economic perspective, whereas $H_2S$ thermal splitting offers a lower SEC. Accordingly, the selection between the two processes depends on minimizing the energy consumption and reducing the overall production cost. These results indicate the need for an integrated techno-economic evaluation when assessing alternative hydrogen production routes from sour gas resources.

## AFFILIATIONS AND AUTHOR DETAILS

### Undergraduate Author

**Zainab Al Abdrabalnabi** – *King Fahd University of Petroleum & Minerals (KFUPM), Dhahran 31261, Saudi Arabia;* 0009-0001-5279-1153
Email: s202154650@kfupm.edu.sa

### Corresponding Author

**Umer Zahid** – *Research Mentor, Interdisciplinary Research Center for Membranes & Water Security, King Fahd University of Petroleum & Minerals (KFUPM), Dhahran 31261, Saudi Arabia;* 0000-0002-9141-1408
Email: uzahid@kfupm.edu.sa

## ACKNOWLEDGMENTS

The authors acknowledge the support provided by the Chemical Engineering Department at King Fahd University of Petroleum and Minerals (KFUPM).

## ETHICS STATEMENT

Not applicable, as this study did not involve human participants, animal subjects, or biological materials.

## COMPETING INTERESTS

The authors declare no competing interests.

## DATA AVAILABILITY

The data supporting the findings of this study are available from the corresponding author upon reasonable request.

## REFERENCES

(1) *Global Energy Review 2025*. www.iea.org.

(2) Al Blooshi, A., Al-Ali, K., AlHajaj, A. & Palmisano, G. Chemical kinetics of two-step thermochemical decomposition of hydrogen sulfide over nickel sulfide. *Int. J. Hydrogen Energy* **52**, 433–446 (2024).

(3) Nailwal, B. C. *et al.* Enhanced H2S decomposition using membrane reactor. *Int. J. Hydrogen Energy* **70**, 251–261 (2024).

(4) Zhu, Y. J., Wan, Y. Y., Tian, Y., Mu, H. M. & Zhang, T. G. Biomass thermal decomposition induced hydrogen sulfide blooming in thermal recovery reservoirs. *Pet. Sci.* **22**, 1802–1810 (2025).

(5) Lou, M. *et al.* Direct H2S Decomposition by Plasmonic Photocatalysis: Efficient Remediation plus Sustainable Hydrogen Production. *ACS Energy Lett.* **7**, 3666–3674 (2022).

(6) Dogan, M. Y., Tasdemir, H. M., Arbag, H., Yasyerli, N. & Yasyerli, S. H2 production via H2S decomposition over activated carbon supported Fe- and W- catalysts. *Int. J. Hydrogen Energy* **75**, 483–495 (2024).

(7) Tollini, F., Sponchioni, M., Calemma, V. & Moscatelli, D. Methane Reforming with H2S and Sulfur for Hydrogen Production: Thermodynamic Assessment. *Energy and Fuels* **37**, 11197–11208 (2023).

(8) Ali, S. M., Alkhatib, I. I. I., AlHajaj, A. & Vega, L. F. Life cycle assessment on the role of H2S-based hydrogen via H2S-methane reforming for the production of sustainable fuels. *Science of The Total Environment* **958**, 177879 (2025).

(9) Abdulrahman, F., Wang, Q., Angikath, F. & Sarathy, S. M. Hydrogen sulfide methane reforming: A kinetic modeling and techno-economic analysis study. *Int. J. Hydrogen Energy* **67**, 750–759 (2024).

(10) Spatolisano, E. *et al.* Hydrogen sulphide to hydrogen via H2S methane reformation: Thermodynamics and process scheme assessment. *Int. J. Hydrogen Energy* **47**, 15612–15623 (2022).

(11) Binoist, M. *et al.* Kinetic study of the pyrolysis of H2S. *Ind. Eng. Chem. Res.* **42**, 3943–3951 (2003).

(12) Spatolisano, E. *et al.* Process sensitivity analysis and techno-economic assessment of hydrogen sulphide to hydrogen via H2S methane reformation. *J. Clean. Prod.* **330**, (2022).

(13) Martínez-Salazar, A. L. *et al.* Hydrogen production by methane and hydrogen sulphide reaction: Kinetics and modeling study over Mo/La2O3-ZrO2 catalyst. in *International Journal of Hydrogen Energy* vol. 40 17354–17360 (Elsevier Ltd, 2015).